Bull. Korean Chem. Soc. **2014**, Vol. 35, No. 7 2019
http://dx.doi.org/10.5012/bkcs.2014.35.7.2019

Electrodeposited NiCu Alloy Catalysts for Glucose Oxidation

Ji-Eun Lim, Sang Hyun Ahn,† Jong Hyun Jang,† Hansoo Park,* and Soo-Kil Kim*

School of Integrative Engineering, Chung-Ang University, Heukseok-dong, Dongjak-gu, Seoul 156-756, Korea
**E-mail: heyshoo@cau.ac.kr (H. Park); sookilkim@cau.ac.kr (S.-K. Kim)*
†Fuel Cell Research Center, Korea Institute of Science and Technology, Seoul 136-791, Korea
Received January 28, 2014, Accepted March 12, 2014

NiCu alloys have been suggested as potential candidates for catalysts in glucose oxidation. In this study, NiCu alloys with different compositions were prepared on a glassy carbon substrate by changing the electrodeposition potential to examine the effect of Ni/Cu ratios in alloys on catalytic activity toward glucose oxidation. Cyclic voltammetry and chronoamperometry showed that NiCu alloys had higher catalytic activity than pure Ni and Cu catalysts. Especially, $Ni_{59}Cu_{41}$ had superior catalytic activity, which was about twice that of Ni at a given oxidation potential. X-ray analyses showed that the oxidation state of Ni in NiCu alloys was increased with the content of Cu by lattice expansion. Ni components in alloys with higher oxidation state were more effective in the oxidation of glucose.

Key Words : Glucose oxidation, NiCu alloy, Catalyst, Activity

Introduction

Hydrogen, in combination with fuel cells, has been proven as an efficient energy-source replacement for fossil fuels without the associated production of toxic components. Accordingly, there have been increasing demands for development of other new fuels such as methanol, ethanol, and formic acid.[1-3] Of those energy sources, a biofuel cell using glucose has emerged as one potential energy source, even though the application of glucose-based biofuel cells has been limited to biosensors and implantable medical devices due to a lower power generation capacity.[4,5] Over the past years, enzymes such as glucose oxidase have been studied as a main biofuel cell catalyst for glucose; however, problems of low stability and poor electron conductivity associated with enzymes have limited their use as commercially available and stable catalysts.[6-8]

Therefore, metal catalysts have been suggested to overcome the disadvantages of enzymes. Gold is considered to be the most powerful metal for glucose oxidation, which has prompted extensive research directed at gold-based catalysts.[9] To maximize their catalytic activities, metal catalysts often require modification by changing the morphology, increasing surface area by incorporation into carbon-based nanomaterials (*e.g.*, carbon nanotubes and graphene), or producing alloy structures with other metal catalysts.[10-14] Tominaga *et al.* compared Au, Ag, and AuAg alloys in alkaline solution, demonstrating that the incorporation of Ag into Au enhanced glucose oxidation.[15] Nanoporous AuAg alloys with different ratios were also examined for catalytic activity toward glucose oxidation.[16] Pt has also been examined as a powerful candidate for glucose oxidation. Cui *et al.* developed PtPb alloy catalysts, which showed enhanced catalytic activity.[10] However, high costs and poisoning either by intermediates during glucose oxidation or by chloride ion under neutral conditions are issues to be resolved before their widespread use as biofuel-cell catalysts can be realized.[8,17]

As alternatives to Au and Pt, Ni and Cu catalysts have recently gained attention as relatively inexpensive metal catalysts for glucose oxidation despite requiring a more positive potential for operation as compared with Au. Yi *et al.* have fabricated Ni nanoflakes on titanium using the hydrothermal method for glucose sensor applications, and reported the sensitivity of Ni nanoflakes as 7.32 mA mM^{-1} cm^{-2}.[18] Huang has reported the fabrication of Ni thin films on a nanoporous Au electrode – using the sequential steps of Zn under-potential deposition and Ni displacement – and their use as catalysts for glucose oxidation.[19] Jafarian *et al.* produced a $Ni_{79}Cu_{21}$ alloy by galvanostatic deposition on glassy carbon for glucose oxidation.[20] The glucose oxidation tests showed that the alloy had a higher catalytic activity than pure Ni; this explained that glucose oxidation occurred during the oxidation of $Ni(OH)_2$, which produced β-NiOOH and γ-NiOOH, and that the higher activity of NiCu alloys was due to the prohibition of γ-NiOOH formation, which could expand and compromise the template, leading to a decrease in catalytic activity.[20] However, a systematic study on the effects of alloy compositions on the catalytic activity of glucose oxidation is rare. Previously, we reported that the modification of a Cu electrode by displacement with Au increased the catalytic activity and lessened the poisoning of catalysts by intermediates during glucose oxidation.[21]

In light of previous findings, the aim of this study is to prepare NiCu alloys with varying ratios and examine their catalytic activities for glucose oxidation. Pure Ni, Cu, and NiCu alloys were deposited onto glassy carbon by electrodeposition; Ni/Cu ratios were controlled by changing the deposition potential. Various electrochemical analytical methods were performed to examine the optimal composition of

NiCu alloy catalysts on glassy carbon.

Experimental

Materials and Chemicals. Glassy carbon (GC) was purchased from HTW Hochtemperatur-Werkstoffe GmbH. $NiSO_4 \cdot 6H_2O$, $CuSO_4 \cdot 5H_2O$ (used for NiCu deposition), $C_6H_5Na_3O_7$ (a complexing agent), and D-(+)-glucose ($C_6H_{12}O_6$) were purchased from Sigma-Aldrich. Sodium hydroxide (NaOH) was purchased from Daejung. Deionized water was used for all experiments. All commercial chemical reagents and solvents were used without additional purification.

Preparation of NiCu Alloys on Glassy Carbon. NiCu alloy was fabricated by electrodeposition using a conventional three-electrode cell. A plate-type glassy carbon substrate, Pt wire, and saturated calomel electrode (SCE, KCl saturated) were used as working, counter, and reference electrodes, respectively. Samples with different ratios of Ni and Cu were fabricated with different deposition potentials (−1.00, −1.05, −1.10, −1.15, −1.20, and −1.35 V) for 2 s using a solution composed of 0.50 M $NiSO_4 \cdot 6H_2O$, 0.05 M $CuSO_4 \cdot 5H_2O$, and 0.26 M $C_6H_5Na_3O_7$ as electrolyte after purging with nitrogen gas. $C_6H_5Na_3O_7$, the complexing agent, was used to prevent solution reaction between the metal precursors having different reduction potentials and to facilitate the alloy composition control. For comparison with pure metals, Ni/GC and Cu/GC were fabricated with a deposition potential of −1.20 V for 2 s.

Characterization of NiCu Alloys on Glassy Carbon. Catalyst compositions were analyzed with electron probe micro analyzer (EPMA, JEOL, JXA-8500F). The sizes, morphologies, and distributions of particles were examined with field-emission scanning electron microscopy (FE-SEM, Hitachi, S-4100). Catalyst crystal structures were obtained using X-ray diffraction (XRD, Rigaku, D/Max 2500) at a scanning rate of 5° per min. The binding energies of Ni in the alloy catalysts were analyzed with X-ray photoelectron spectroscopy (XPS, PHI, 5800 ESCA).

Cyclic voltammetry (CV) and chronoamperometry (CA) were performed using a three-electrode system connected to a potentiostat/galvanostat (Autolab, PGSTAT302F) to evaluate glucose oxidation activities of the prepared catalysts. The same counter and reference electrodes used for electrodeposition were used in the glucose oxidation tests. NaOH solutions (0.3 M) containing different concentrations of glucose (0, 5, 10, 15, and 20 mM) were used as electrolytes. CV scans were performed in the potential range from −0.4 to 0.8 V at a scan rate of 50 mV s^{-1} in both the forward and backward directions. CA data were collected in 0.3 M NaOH aqueous solution containing 15 mM of glucose at 0.6 V for 3600 s.

Results and Discussion

Figure 1 shows FE-SEM images of pure Cu and one of the NiCu alloys deposited on glassy carbons; SEM images for Ni and various samples of NiCu alloys ($Ni_{16}Cu_{84}$, $Ni_{23}Cu_{77}$, $Ni_{40}Cu_{60}$, $Ni_{51}Cu_{49}$, $Ni_{59}Cu_{41}$) can be found at the authors' previous work on NiCu alloy catalysts for the cathode reaction (hydrogen evolution) of alkaline water splitting.[22] The coverage of Cu deposited at −1.20 V appeared higher than that of Ni deposited at the same potential (Figure 1(a) *vs.* Figure 2(a) of ref. 22, respectively) because of differences in the standard reduction potentials (0.34 *vs.* −0.25 V). Some aggregates were also observed in pure Cu sample. In general, in the case of NiCu alloys, surface coverage was gradually increased as deposition potential was negatively shifted to −1.35 V, with a simultaneous decrease in particle size.[22] However, no hierarchical structures that might significantly affect the geometric surface area were observed. Notably, NiCu alloy ($Ni_{64}Cu_{36}$) deposited at −1.35 V (Figure 1(b)) showed poor adhesion due to mass-transfer limitations and hydrogen evolution during electrodeposition at this highly negative potential.

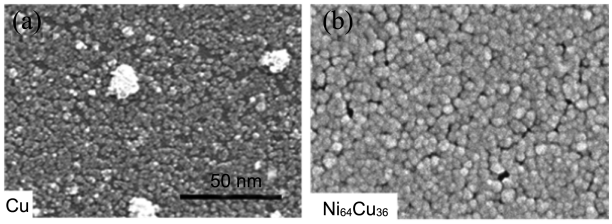

Figure 1. FE-SEM images of (a) Cu deposited at −1.20 V and (b) NiCu alloy deposited at −1.35 V. The SEM images of the rest of electrodeposited catalysts, that is, Ni deposited at −1.20 V and NiCu alloys deposited at −1.20 V, −1.15 V, −1.10 V, −1.05 V, and −1.00 V can be found at authors' previous work.[22]

Composition analysis for each samples indicated that the Ni contents increased with negative potentials. In our preliminary experiments with linear sweep voltammetry (LSV), the reduction of Ni was affected more by negative potentials than that of Cu, resulting in greater Ni deposition with an increase in negative potentials. From the XRD analysis of our previous work[22] and more samples of this work, as Cu content was increased (at more positive deposition potential), the (111) peak position shifted from Ni (111) to Cu (111) because of the lattice expansion resulting from Cu having a larger lattice parameter, confirming the fabrication of NiCu alloys.

After this brief consideration toward NiCu alloy fabrication, the detailed description of which can be found in our previous work,[22] we applied the alloys to glucose oxidation. Figure 2 shows CVs of Ni, Cu and NiCu alloys in 0.3 M NaOH solution without glucose for examining their oxidation–reduction reactions. In the case of Ni, peaks at +0.4 V in a forward line (oxidation) and at +0.34 V in a backward line (reduction) were present, which correspond to the Ni(II)–Ni(III) redox couple involving NiOOH.[20] The oxidation peak for NiCu alloys was shifted to a higher position (+0.43 V) than that for pure Ni, implying the complex behaviors of NiOOH formation on NiCu alloys. In the case of Cu, no sign of redox peaks relevant to the oxide/hydroxide was observed, of which the reason was discussed in the next paragraph in combination with the glucose

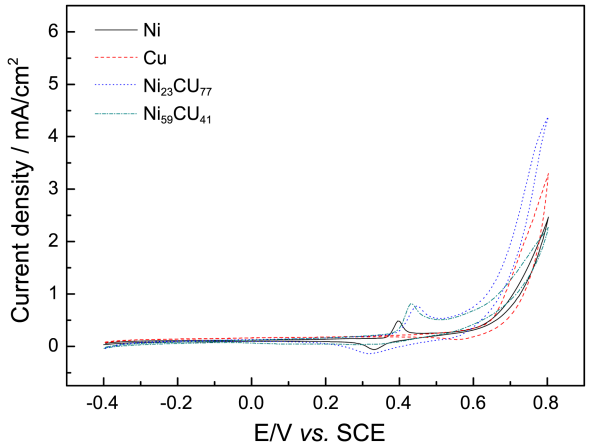

Figure 2. Cyclic voltammetry of Ni, Cu, and NiCu alloys of varying compositions in 0.3 M NaOH. The scan rate is 50 mV s^{-1}.

oxidation. The rapid increase in the current at potentials higher than +0.6 V for NiCu alloys involved either the generation of oxygen through water splitting or formation of Cu(III) oxide/hydroxide; however, since there was no reduction peak of CuO(OH) to $Cu(OH)_2$ during the backward scan,[21] it is reasonable to attribute the peak to oxygen evolution. Notably, NiCu alloys have a lower onset potential of oxygen evolution than that of pure Ni, suggesting the possibility of NiCu alloys as anode catalysts for alkaline water splitting.

To examine the catalytic activity of NiCu alloys toward glucose oxidation, CVs were recorded in 0.3 M NaOH containing 15 mM glucose. As shown in Figure 3(a), while pure Cu deposited at −1.20 V showed a negligible glucose oxidation activity, the Ni catalyst deposited at the same potential showed an onset potential of glucose oxidation at +0.3 V with a peak potential of +0.55 V and peak current of 2.9 mA cm^{-2}. Most of NiCu alloy catalysts exhibited better activity in glucose oxidation than pure Ni, and the onset potentials and peak currents were a strong function of alloy composition. For example, $Ni_{64}Cu_{36}$ alloys fabricated at −1.35 V had an onset potential of glucose oxidation at +0.25 V (*ca.* 50 mV more negative than pure Ni) and a peak potential of +0.65 V with a peak current of 5.2 mA cm^{-2}. Since the peaks attributable to the catalyst surface oxidation (NiOOH formation) and oxygen evolution during the glucose oxidation test were buried in the major peak, it would be more precise to compare current densities at +0.6 V for the evaluation of catalytic activities. The current densities at +0.6 and +0.7 V are summarized in Figures 3(b) and (c). However, before activities can be compared, it is necessary to explain the inactivity of pure Cu deposits, which is contrary to a previous finding.[21,23] We believed that this poor activity might be due to the different morphologies and amounts of Cu; accordingly, samples fabricated at different deposition times were examined. Figure 3(d) presents the CVs of Cu deposited on glassy carbon for 1, 2, 5, and 10 s at −1.2 V. As expected, similar behaviors of Cu oxide/hydroxide formation and glucose oxidation to our

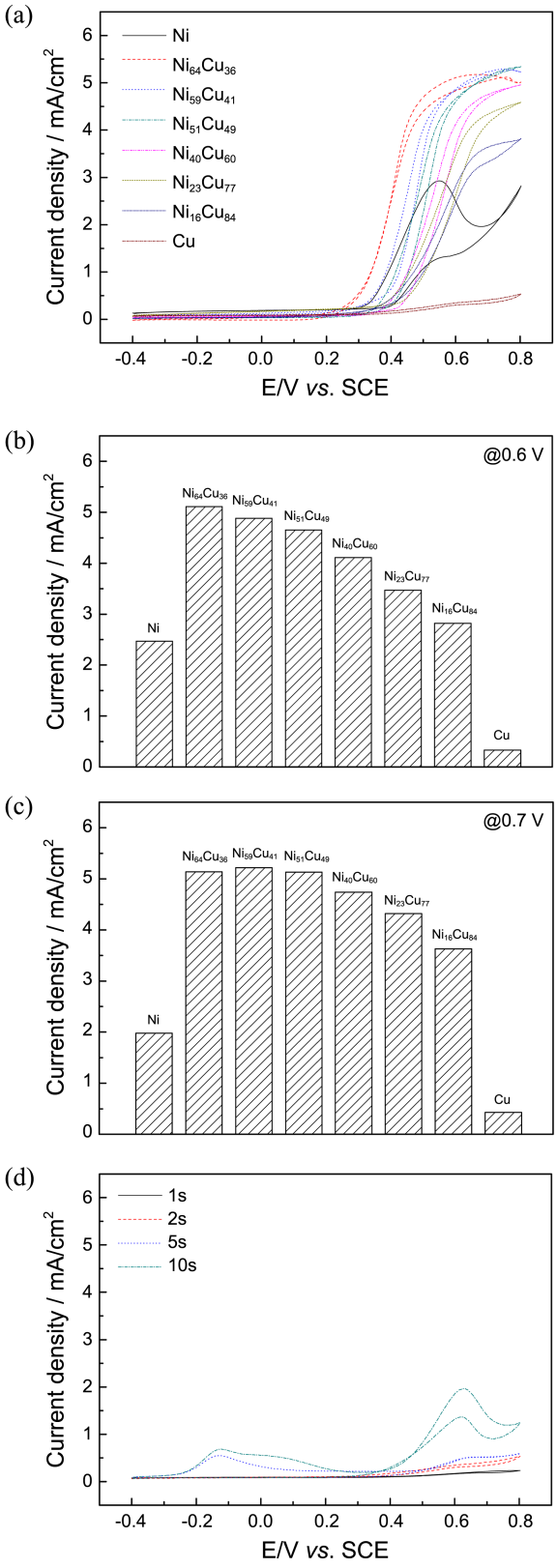

Figure 3. (a) CVs of Ni, Cu, and NiCu alloys of varying compositions in 15 mM glucose and 0.3 M NaOH. The scan rate is 50 mV s^{-1}. Current densities for glucose oxidation for NiCu alloys with varying compositions at (b) +0.6 V and (c) +0.7 V (from (a)) are presented. (d) CVs of Cu deposits with different deposition times in 15 mM glucose and 0.3 M NaOH. The scan rate is 50 mV s^{-1}.

previous results with Cu foil[21] were observed as deposition time was increased up to more than 5 s.

Based on these findings, we hypothesized that the increase in catalytic activity of NiCu alloys deposited for 2 s was not associated with the individual effects of Ni and Cu. Instead, Ni probably worked as a main catalyst for glucose oxidation and Cu enhanced the activity of Ni in the alloy.

By referring to the comparison of current densities of each sample at +0.6 V *vs.* SCE in Figure 3(b), it is evident that NiCu alloys had a significantly higher current than Ni or Cu only. Small amounts of Ni contents, *i.e.*, 16% Ni, enabled the dramatic increase in activity compared to pure Cu. The activities were gradually increased with increase in Ni content, with $Ni_{64}Cu_{36}$ showing the highest value. All alloy catalysts exhibited a higher activity than pure Ni. However, as indicated in an earlier section, because $Ni_{64}Cu_{36}$ catalyst showed poor adhesion on GC, severe delamination was observed after the activity test. It is also noted that at a higher oxidation potential (+0.7 V) shown in Figure 3(c), the $Ni_{59}Cu_{41}$ catalyst exhibited the highest activity, although the difference with $Ni_{64}Cu_{36}$ was insignificant. However, no adhesion problems were observed for $Ni_{59}Cu_{41}$, which enables the utilization of $Ni_{59}Cu_{41}$ catalyst as an effective physically stable catalyst for glucose oxidation within a wide oxidation potential range.

The enhanced catalytic activities of the alloy catalysts are likely due to electron transfer between Ni and Cu components caused by the changes in lattice parameters. Notably, the electronegativities of the two metals are almost the same (1.91 *vs.* 1.90). As shown in Figure 4, XPS analysis revealed the occurrence of electron transfer processes in the catalysts; the binding energies of 2p electrons of Ni, $Ni_{59}Cu_{41}$, and $Ni_{64}Cu_{36}$ are illustrated. Here, the Ni^0 and Ni^0 satellite peaks are located at 852.6 and 854.2 eV, respectively, while the $Ni(OH)_2$ and $Ni(OH)_2$ satellite peaks appear at 856.1 and 861.1 eV, respectively.[24] There is also the possibility that the binding energies higher than 852.6 eV might correspond to the peaks attributable to NiOOH, NiO, and $Ni(OH)_2$.[25] The amounts of Ni^0 in alloys were observed to decrease whereas the amounts of Ni in higher oxidation states were increased as compared to those in Ni deposits. This result indicates

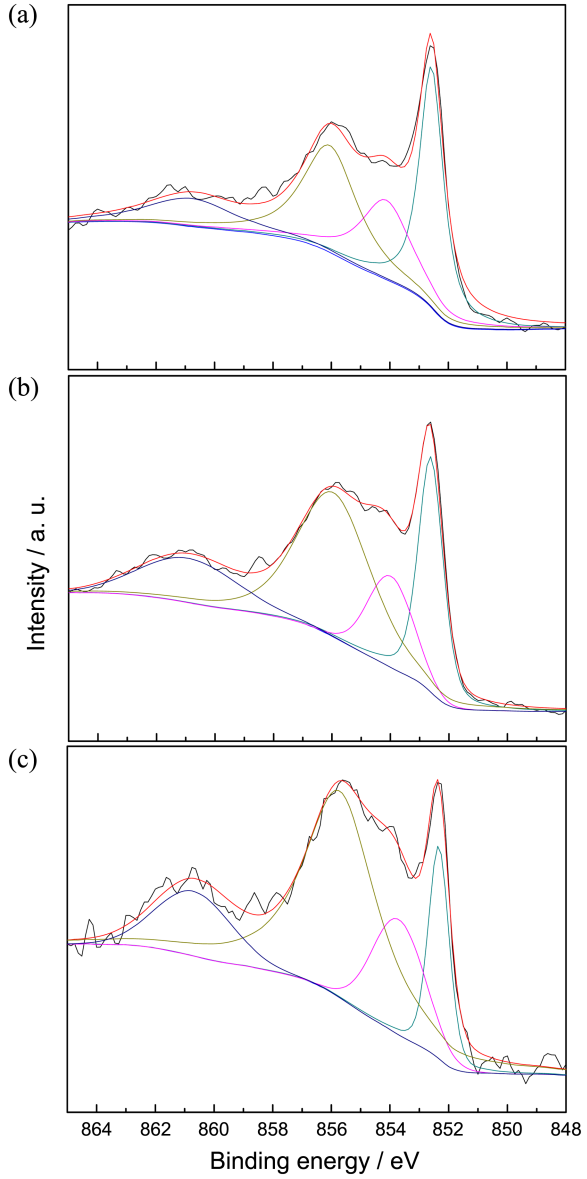

Figure 4. Ni 2p binding energies of (a) Ni, (b) $Ni_{59}Cu_{41}$, and (c) $Ni_{64}Cu_{36}$.

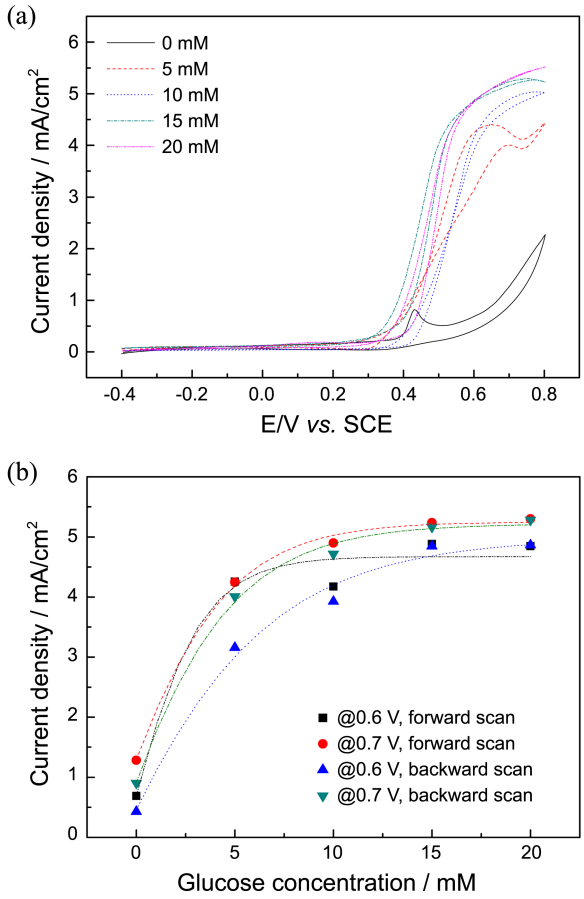

Figure 5. (a) CVs of glucose oxidation using $Ni_{59}Cu_{41}$ with various concentrations (0, 5, 10, 15, 20 mM) of glucose in 0.3 M NaOH and (b) the calibration curves of CV results. The scan rate is 50 mV s^{-1}.

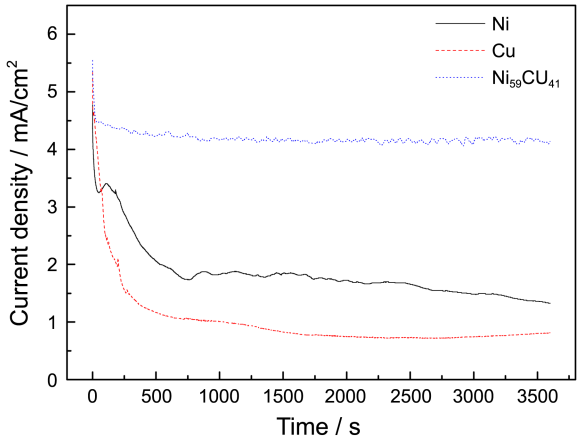

Figure 6. Chronoamperogram of glucose oxidation at +0.6 V according to the types of the electrodes (Ni, Cu, and $Ni_{59}Cu_{41}$ alloy). The electrolyte is composed of 15 mM glucose and 0.3 M NaOH.

that the increase in Cu content increased the lattice parameters of NiCu alloys, leading to the depletion of electrons and increase in the oxidation state of Ni. The very small difference in electronegativities may have an insignificant effect on the electron transfer. The higher oxidation states serve to enhance the capability of Ni within the NiCu alloys to accept electrons produced by glucose oxidation. Notably, we have observed the strong segregation of Ni on the surface of NiCu alloys through a comparison of surface and bulk compositions measured by CV and inductively coupled plasma mass spectroscopy.[22] Exposure of more Ni on the surface may contribute in part to the enhanced activity.

Figure 5(a) shows the CVs of glucose oxidation using $Ni_{59}Cu_{41}$ as a function of glucose concentration (0, 5, 10, 15, and 20 mM). It was found that the currents at +0.6 V increased with glucose concentrations in a forward direction up to 15 mM. A high concentration of glucose, *i.e.*, 20 mM, showed no difference from 15 mM. This result could be explained by the slower reaction rate of glucose as compared to that of other species such as ascorbic acid,[26] resulting in a limitation in the number of active sites and saturation. The saturation behavior is more obvious in Figure 5(b), which is the calibration curve of Figure 5(a) obtained at two different potentials of +0.6 V and +0.7 V for both forward and backward scans.

Chronoamperometry was conducted to examine the stability of the prepared catalysts. Figure 6 shows the results for Ni, Cu, and $Ni_{59}Cu_{41}$ in 0.3 M NaOH solution containing 15 mM glucose at +0.6 V for 3600 s. All samples had an abrupt decrease in stability until 500 s, followed by a gradual decrease. The results also confirmed the higher activity and better stability of NiCu alloys than those of Ni or Cu alone.

Conclusion

NiCu alloys with different compositions were fabricated on glassy carbon substrates by changing electrodeposition potential. Alloy formation and the catalytic activities were studied using various analytical techniques. The fabricated NiCu alloys showed a much higher catalytic activity than pure Ni or Cu toward glucose oxidation. The most suitable alloy catalyst having high activity and physical stability was $Ni_{59}Cu_{41}$. XPS results revealed that the oxidation state of Ni in NiCu alloys was higher than that of the Ni deposit because of lattice expansion by the addition of Cu in alloys. Thus, the electron-depleted state of NiCu alloys accelerated the acceptance of electrons during glucose oxidation.

Acknowledgments. This research was supported by the Basic Science Research Program through the National Research Foundation of Korea (NRF) funded by the Ministry of Education, Science, and Technology (2012R1A1A1004731). This work was also financially supported by KIST Institutional Program (2E24841).

References

1. Liu, H.; Song, C.; Zhang, L.; Zhang, J.; Wang, H.; Wilkinson, D. P. *J. Power Sources* **2006**, *155*, 95.
2. Rice, C.; Ha, S.; Masel, R. I.; Waszczuk, P.; Wieckowski, A.; Barnard, T. *J. Power Sources* **2002**, *111*, 83.
3. Vigier, F.; Coutanceau, C.; Perrard, A.; Belgsir, E. M.; Lamy, C. *J. Appl. Electrochem.* **2004**, *34*, 439.
4. Barton, S. C.; Gallaway, J.; Atanassov, P. *Chem. Rev.* **2004**, *104*, 4867.
5. Bullen, R. A.; Arnot, T. C.; Lakeman, J. B.; Walsh, F. C. *Biosens. Bioelectron.* **2006**, *21*, 2015.
6. Park, S.; Boo, H.; Chung, T. D. *Anal. Chim. Acta* **2006**, *556*, 46.
7. Rong, L.-Q.; Yang, C.; Qian, Q.-Y.; Xia, X.-H. *Talanta* **2007**, *72*, 819.
8. Toghill, K. E.; Compton, R. G. *Int. J. Electrochem. Sci.* **2010**, *5*, 1246.
9. Wang, J. F.; Gong, J. X.; Xiong, Y. S.; Yang, J. D.; Gao, Y.; Liu, Y. L.; Lu, X. Q.; Tang, Z. Y. *Chem. Commun.* **2011**, 6894.
10. Cui, H. F.; Ye, J. S.; Liu, X.; Zhang, W. D.; Sheu, F. S. *Nanotechnol.* **2006**, *17*, 2334.
11. Hu, Y.; Jin, J.; Wu, P.; Zhang, H.; Cai, C. *Electrochim. Acta* **2010**, *56*, 491.
12. Mahshid, S. S.; Mahshid, S.; Dolati, A.; Ghorbani, M.; Yang, L.; Luo, S.; Cai, Q. *Electrochim. Acta* **2011**, *58*, 551.
13. Sun, Y. P.; Buck, H.; Mallouk, T. E. *Anal. Chem.* **2001**, *73*, 1599.
14. Wang, G. F.; Wei, Y.; Zhang, W.; Zhang, X. J.; Fang, B.; Wang, L. *Microchimica. Acta* **2010**, *168*, 87.
15. Tominaga, M.; Shimazoe, T.; Nagashima, M.; Kusuda, H.; Kubo, A.; Kuwahara, Y.; Taniguchi, I. *J. Electroanal. Chem.* **2006**, *590*, 37.
16. Liu, Z.; Huang, L.; Zhang, L.; Ma, H.; Ding, Y. *Electrochim. Acta* **2009**, *54*, 7286.
17. Holt-Hindle, P.; Nigro, S.; Asmussen, M.; Chen, A. *Electrochem. Commun.* **2008**, *10*, 1438.
18. Yi, Q.; Huang, W.; Yu, W.; Li, L.; Liu, X. *Electroanalysis* **2008**, *20*, 2016.
19. Huang, J. F. *Chem. Commun.* **2009**, 1270.
20. Jafarian, M.; Forouzandeh, F.; Danaee, I.; Gobal, F.; Mahjani, M. G. *J. Solid State Electrochem.* **2009**, *13*, 1171.
21. Lim, J.-E.; Ahn, S. H.; Pyo, S. G.; Son, H.; Jang, J. H.; Kim, S.-K. *Bull. Korean Chem. Soc.* **2013**, *34*, 2685.
22. Ahn, S. H.; Park, H.-Y.; Choi, I.; Yoo, S. J.; Hwang, S. J.; Kim, H.-J.; Cho, E.; Yoon, C. W.; Park, H.; Son, H.; Hernandez, J. M.; Nam, S. W.; Lim, T.-H.; Kim, S.-K.; Jang, J. H. *Int. J. Hydrogen Energy* **2013**, *38*, 13493.
23. Hassan, H. B.; Hamid, Z. A. *Int. J. Electrochem. Sci.* **2011**, *6*,

5741.
24. Nesbitt, H. W.; Legrand, D.; Bancroft, G. M. *Phys. Chem. Minerals* **2000**, *27*, 357.
25. Biesinger, M. C.; Payne, B. P.; Lau, L. M. W.; Gerson, A.; Smart, R. St. C. *Surf. Interface. Anal.* **2000**, *41*, 324.
26. Park, D. J.; Lee, Y. J.; Park, J. Y. *J. Semicond. Sci. Technol.* **2007**, *7*, 161.